nature chemical biology

Chemical inhibitor of nonapoptotic cell death with therapeutic potential for ischemic brain injury

Alexei Degterev[1], Zhihong Huang[2], Michael Boyce[1], Yaqiao Li[1], Prakash Jagtap[3], Noboru Mizushima[4], Gregory D Cuny[3], Timothy J Mitchison[5], Michael A Moskowitz[2] & Junying Yuan[1]

The mechanism of apoptosis has been extensively characterized over the past decade, but little is known about alternative forms of regulated cell death. Although stimulation of the Fas/TNFR receptor family triggers a canonical 'extrinsic' apoptosis pathway, we demonstrated that in the absence of intracellular apoptotic signaling it is capable of activating a common nonapoptotic death pathway, which we term necroptosis. We showed that necroptosis is characterized by necrotic cell death morphology and activation of autophagy. We identified a specific and potent small-molecule inhibitor of necroptosis, necrostatin-1, which blocks a critical step in necroptosis. We demonstrated that necroptosis contributes to delayed mouse ischemic brain injury *in vivo* through a mechanism distinct from that of apoptosis and offers a new therapeutic target for stroke with an extended window for neuroprotection. Our study identifies a previously undescribed basic cell-death pathway with potentially broad relevance to human pathologies.

The caspase family of cysteine proteases has an indispensable role in the signal transduction and execution of apoptosis[1]. Stimulation of the Fas/TNFR family of death-domain receptors (DRs) by their corresponding ligands activates a canonical apoptotic pathway that includes a sequential activation of multiple caspases[2]. Paradoxically, however, a growing number of studies has reported that caspase inhibition does not prevent DR-induced cell death. Furthermore, cell death induced under such conditions lacks the typical features of apoptosis and instead resembles necrosis[3–6]. For example, FasL, TNFα and TRAIL induced the necrotic cell death of Jurkat cells in the presence of the pan-caspase inhibitor zVAD.fmk[6]. In Jurkat cells deficient for either the adaptor molecule FADD or caspase-8, two critical upstream activators of apoptotic signaling, TNFα stimulation directly leads to necrotic cell death[4,6–8]. Inhibition of caspases also does not block DR agonist–induced cell death and leads to necrosis of NIH3T3 cells[9], mouse embryonic fibroblasts (MEFs)[10], U937 monocytic cells[9], and IEC-6 (ref. 11) and HT29 (ref. 12) epithelial cells.

The similar necrotic morphological features shown by multiple cell types when undergoing DR-induced cell death without caspase activation suggest the presence of a shared, alternative, nonapoptotic cell-death pathway. However, it is unclear whether these observations in disparate systems are the results of a single common mechanism, nor are there tools to distinguish such a pathway from other types of cellular demise. Furthermore, the pathophysiological relevance of the DR-induced nonapoptotic death *in vivo*, if any, remains completely unknown.

Necrotic cell death is common in a wide variety of pathological conditions[13], including stroke[14]. Very little attempt, however, has been made to develop therapeutics to specifically target necrosis because of the conventional notion that, unlike apoptosis, necrotic cell death is a nonregulated response to overwhelming stress. The demonstration of a common necrotic cell-death pathway activated by a classical DR signal in the absence of any cellular damage directly challenges this notion and suggests that a portion of necrotic cell death *in vivo* might in fact be regulated by cellular machinery. This, in turn, may provide an unprecedented opportunity to selectively target pathological necrotic cell death.

Here, we used small molecules to define the nonapoptotic pathway mediated by DRs in the absence of caspase signaling. We identified necrostatin-1 (Nec-1, **1**), a specific and potent small-molecule inhibitor of cell death caused by DR stimulation in the presence of caspase inhibition in multiple cell types. These results provide the first direct evidence that DR signaling triggers a common alternative nonapoptotic cell-death pathway, which we term necroptosis. Using Nec-1 (see **Supplementary Methods** online for details of the structure and preparation of this compound and its derivatives), we demonstrated that necroptosis is a delayed component of ischemic neuronal injury and may therefore represent a promising therapeutic target for the treatment of stroke.

[1]Department of Cell Biology, Harvard Medical School, 240 Longwood Avenue, Boston, Massachusetts 02115, USA. [2]Stroke and Neurovascular Regulation Laboratory, Massachusetts General Hospital, Harvard Medical School, 149 13th Street, Charlestown, Massachusetts 02129, USA. [3]Laboratory for Drug Discovery in Neurodegeneration, Harvard Center for Neurodegeneration and Repair, Brigham & Women's Hospital and Harvard Medical School, 65 Landsdowne St., Cambridge, Massachusetts 02139, USA. [4]Department of Bioregulation and Metabolism, The Tokyo Metropolitan Institute of Medical Science, 3-18-22 Honkomagome, Bunkyo-ku, Tokyo 113-8613, Japan. [5]Department of Systems Biology, Harvard Medical School, 240 Longwood Avenue, Boston, Massachusetts 02115, USA. Correspondence should be addressed to J.Y. (jyuan@hms.harvard.edu).

Published online 29 May 2005; doi:10.1038/nchembio711

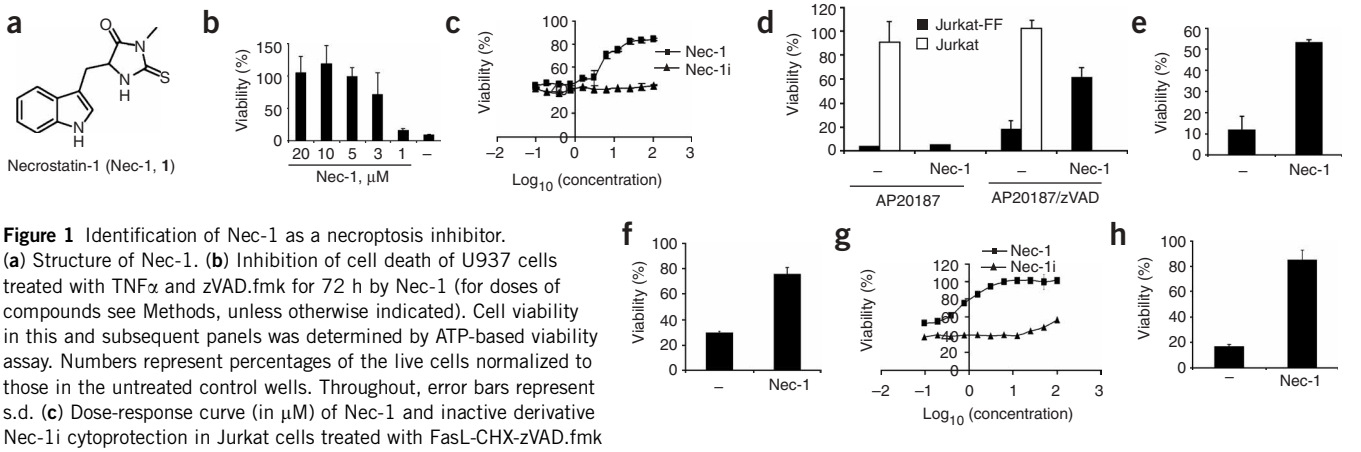

Figure 1 Identification of Nec-1 as a necroptosis inhibitor. (**a**) Structure of Nec-1. (**b**) Inhibition of cell death of U937 cells treated with TNFα and zVAD.fmk for 72 h by Nec-1 (for doses of compounds see Methods, unless otherwise indicated). Cell viability in this and subsequent panels was determined by ATP-based viability assay. Numbers represent percentages of the live cells normalized to those in the untreated control wells. Throughout, error bars represent s.d. (**c**) Dose-response curve (in μM) of Nec-1 and inactive derivative Nec-1i cytoprotection in Jurkat cells treated with FasL-CHX-zVAD.fmk for 30 h. Numbers represent viability normalized to that of the corresponding compound-treated cells in the absence of FasL. (**d**) Inhibition of cell death in Jurkat cells stably expressing dimerizable FADD (Jurkat-FF) by Nec-1 after treatment with dimerizer AP20187 and zVAD.fmk for 48 h. Numbers represent viability normalized to that of the corresponding compound-treated cells in the absence of dimerizer. In addition, control Jurkat cells were also treated with AP20187 in the presence or absence of zVAD.fmk without Nec-1. (**e**,**f**,**h**) Inhibition of cell death in BALB/c 3T3 (**e**), SV40-transformed MEF (**f**) and L929 (**h**) cells by Nec-1. Cells were treated with TNFα (**e**,**f**,**h**), zVAD.fmk (**e**,**f**) and CHX (**f**) for 16 (**f**) or 24 (**e**,**h**) h. Numbers represent viability normalized to that of the compound-treated cells in the absence of TNFα. (**g**) Dose response of Nec-1 and Nec-1i cytoprotection of FADD-deficient Jurkat cells treated with TNFα for 30 h (see **c** for conditions).

RESULTS

Identification of necrostatin-1

Because chemical inhibitors of caspases have been instrumental in the characterization of apoptosis in mammalian systems, we expected that specific necroptotic inhibitors would be equally useful for demonstrating the existence of a common, alternative cell-death pathway in multiple cell types, for providing specific tools to distinguish necroptosis from other cell-death processes, and as potential lead molecules targeting the nonapoptotic component of pathologic cell death for therapeutic benefit. We screened a chemical library of ~15,000 compounds for chemical inhibitors of the necrotic death of human monocytic U937 cells induced by TNFα and zVAD.fmk[15], which we used as an operational definition of necroptosis. This screen resulted in the selection of Nec-1, which efficiently blocked necroptotic death in U937 cells in a concentration-dependent fashion (**Fig. 1a**,**b**).

Next, we used Nec-1 as a tool to examine whether the DR-induced nonapoptotic cell death observed in disparate cell types is mediated by a common mechanism. Nec-1 inhibited all published examples of necrotic cell death induced by DR activation in the presence of caspase inhibitors, including the necrotic death of (i) Jurkat cells induced by FasL, cycloheximide (CHX) and zVAD.fmk (FasL-CHX-zVAD.fmk[6], **Fig. 1c**), (ii) Jurkat cells stably expressing FADD fused to the FKBP12-based dimerization domain (JK-FF) in the presence of chemical dimerizer AP20187 and zVAD.fmk[4] (**Fig. 1d**), (iii) BALB/c 3T3 cells[15] treated with TNFα and zVAD.fmk (TNFα-zVAD.fmk) or FasL and zVAD.fmk (FasL-zVAD.fmk, **Fig. 1e**), and (iv) MEF[10] (**Fig. 1f**), HT29 (ref. 12), and IEC-18 and HL-60 cells treated with TNFα-zVAD.fmk (data not shown).

Although Nec-1 was selected in a screen with zVAD.fmk, its action is not dependent upon pharmacological inhibition of caspases. Consistent with the direct activation of necroptosis, Nec-1 prevented the death of TNFα-treated FADD-deficient Jurkat cells, which are unable to activate caspases in response to DR signaling[7], even in the absence of zVAD.fmk (**Fig. 1g**). Similarly, Nec-1 efficiently inhibited the TNFα-induced necrotic death of L929 cells, which does not require exogenous caspase inhibitors[5] (**Fig. 1h**). Overall, the ability of Nec-1 to inhibit cell death in all of these systems provides the first direct demonstration of the existence of a common necroptotic pathway mediated by DR signaling. Because the induction of necroptosis in FADD-deficient Jurkat cells does not rely on the presence of other chemicals (CHX, zVAD.fmk), we used this system to determine the effective concentration for half-maximum response (EC_{50}) for Nec-1 of 494 ± 125 nM (**Fig. 1g**). Efficient protection from necroptosis by Nec-1 was confirmed by several different assays, including forward- and side-scatter analyses of cell size (**Supplementary Fig. 1** online), ATP level (**Fig. 1**), mitochondrial dysfunction (**Fig. 2a**,**b** and data not shown), plasma membrane permeabilization (**Fig. 2a–c** and data not shown) and cell proliferation (**Supplementary Fig. 1**). Consistent with these results, morphological analyses based on electron, fluorescent and bright-field microscopy demonstrated that Nec-1 inhibited all manifestations of necroptotic cell death (**Fig. 2d–f** and **Supplementary Figs. 1** and **2** online). These results establish Nec-1 as a potent and efficient inhibitor of necroptosis.

Specificity of Nec-1

To establish the specificity of Nec-1, we compared its effects on DR-induced apoptosis as compared to necroptosis, which can be readily distinguished by morphological criteria and selective dye staining. Nec-1 had no effect on FasL-CHX–induced accumulation of annexin V–positive and propidium iodide (PI)–negative cells, a result indicative of apoptosis[16] (**Fig. 3a**). Conversely, Nec-1 efficiently inhibited the simultaneous loss of mitochondrial membrane potential and plasma membrane integrity in FADD-deficient Jurkat cells treated with TNFα (**Fig. 2a**) or wild-type Jurkat cells treated with FasL-CHX-zVAD.fmk (**Fig. 2b**). The onset of apoptosis was notably faster than that of necroptosis in response to the similar stimuli (FasL-CHX and FasL-CHX-zVAD.fmk, respectively; see **Figs. 2b** and **3a**), which might suggest that apoptosis usually masks or preempts necroptosis in this cell type because of its faster kinetics.

Consistent with this observation, Nec-1 had no effect on apoptotic morphology (cytoplasm condensation, chromatin marginalization, nuclear fragmentation and plasma membrane blebbing) in FasL-CHX–treated apoptotic Jurkat cells (**Fig. 2f**), whereas it completely inhibited the appearance of necrotic morphology (nuclear condensation, organelle swelling, early loss of plasma membrane integrity and

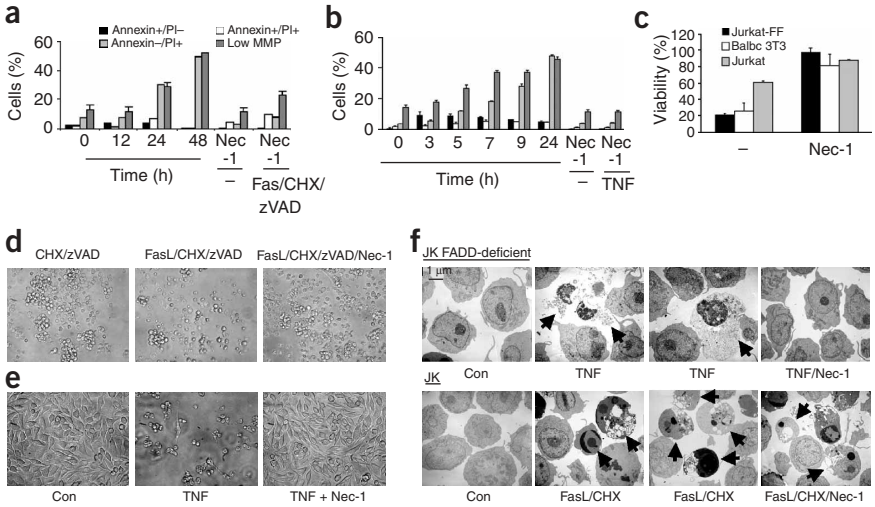

Figure 2 Efficient inhibition of all manifestations of necroptosis by Nec-1. (**a**,**b**) Inhibition of plasma membrane integrity loss and mitochondrial dysfunction by Nec-1. Wild-type (**a**) and FADD-deficient (**b**) Jurkat cells were treated with FasL-CHX-zVAD.fmk (**a**) or with TNFα (**b**) for the indicated amounts of time. Where indicated, the cells were also treated with Nec-1 for 24 h. Cells were stained with $DiOC_6$ or with annexin V and PI, and percentages of cells with low PI and high annexin V, high PI and high annexin V, high PI and low annexin V, and low $DiOC_6$ (low mitochondrial membrane potential) are shown. Throughout, error bars represent s.d. (**c**) Demonstration of Nec-1 suppression of necroptosis from Sytox assay. Jurkat-FF cells were treated with AP20187-zVAD.fmk and Nec-1 for 48 h. Values represent the percentages of live cells normalized to the compound-treated cells lacking dimerizer. Alternatively, BALB/c 3T3 cells were treated with TNFα-zVAD.fmk and 40 μM Nec-1 for 24 h, or Jurkat cells were treated with FasL-CHX-zVAD.fmk and Nec-1 for 48 h. (**d**,**e**) Bright-field microscopy of the cytoprotective effect of Nec-1 in (**d**) Jurkat cells treated with FasL-CHX-zVAD.fmk or (**e**) L929 cells treated with TNFα for 36 h. Bright-field images were acquired at 40× magnification. (**f**) Electron microscopy of the effect of Nec-1 in apoptotic or necroptotic Jurkat cells treated with FasL and CHX for 16 h or TNFα for 6 h, respectively. Representative EM images are shown. Arrows indicate dead cells. Con, vehicle-only control.

the appearance of translucent cytosol; see **Fig. 2d**,**f**) in TNFα-treated, FADD-deficient Jurkat cells[7]. Selective protection from necroptosis induced by DR signaling was also observed in other cell-death assays (**Figs. 1d** and **3b**,**c** and data not shown). These results establish the selectivity of Nec-1 in inhibiting necroptosis and point to the divergent regulation of these two types of cell death. Consistent with this model, overexpression of Bcl-x_L in Jurkat cells, which potently suppressed apoptosis, did not inhibit necroptosis (data not shown).

To further establish the specificity of Nec-1, we analyzed its possible effect on other cell physiological parameters. We found that Nec-1 had no general effect in healthy cells on ATP levels, mitochondrial membrane potential, plasma membrane integrity, cell shape or size, cell cycle distribution, proliferation, global mRNA expression as reflected in Agilent mRNA chip analysis, the intracellular levels of reactive oxygen species (ROS), cell adhesion, actin and microtubule cytoskeletons, or the morphology of various cellular compartments, for example, nuclei, Golgi apparatus, endoplasmic reticulum and mitochondria (**Supplementary Figs. 1** and **2**). These observations suggest that Nec-1 is specific for necroptosis. To further characterize the specificity of Nec-1, we performed extensive structure-activity relationship analyses and found that most of the 93 chemical modifications of Nec-1 that we tested resulted in either substantial or complete loss of activity (data not shown). For example, elimination of the methyl group in the hydantoin moiety (Nec-1i, **2**; **Fig. 3d** and **Supplementary Methods**) completely abolished antinecroptotic activity (**Fig. 1c**,**g**). Of all Nec-1 modifications tested, only two types of changes preserved its antinecroptotic activity. First, the addition of a chlorine to the phenyl ring of Nec-1 (7-Cl-Nec-1, **3**; **Fig. 3d** and **Supplementary Methods**) resulted in an approximately 2.7-fold increase in activity (EC_{50} = 182 ± 24 nM). Second, changing the sulfur in the hydantoin moiety, which is a potential metabolic liability, to oxygen did not affect the antinecroptotic activity of Nec-1 (7-Cl-O-Nec-1, **4**; **Fig. 3d** and **Supplementary Methods**; EC_{50} = 206 ± 33 nM). Such stringent structural requirements point to the highly specific mode of necrostatin cytoprotection.

Finally, we compared the activity of Nec-1 to that of other small-molecule regulators of cellular signaling. Our analyses revealed that necroptotic cell death in Jurkat and BALB/c 3T3 cells cannot be blocked by small-molecule inhibition of such factors as the mitochondrial permeability transition pore, calpains, calcium homeostasis perturbation, poly(ADP-ribose) polymerase (PARP), HtrA2/Omi, phospholipase A2 and nitric oxide synthase, or the RNAi-mediated downregulation of apoptosis-inducing factor (data not shown). Furthermore, we screened a chemical library of 489 compounds with

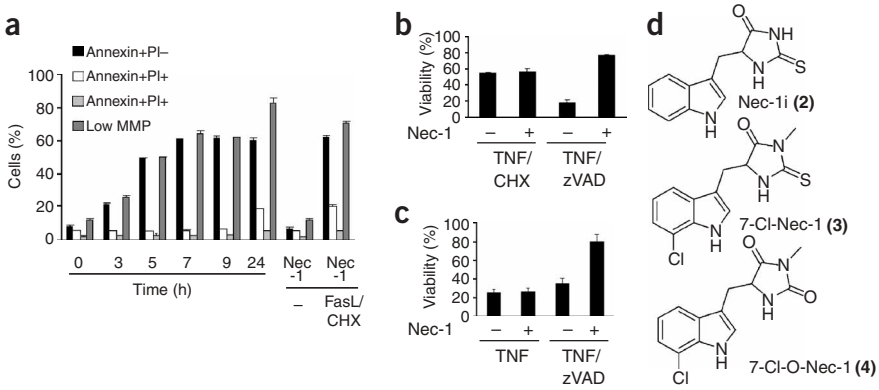

Figure 3 Specificity of Nec-1. (**a**) Lack of cytoprotection by Nec-1 in apoptotic Jurkat cells treated with FasL-CHX for 24 h. Time course of cellular changes in the samples not treated with Nec-1 is also shown. Cells were stained with $DiOC_6$ or annexin V and EGFP-PI as described in **Figure 2a**,**b**. (**b**,**c**) Selective inhibition of necroptosis but not apoptosis by Nec-1 in U937 (**b**) and BALB/c 3T3 (**c**) cells treated with TNFα and CHX (**b** only) without (apoptosis) or with (necroptosis) zVAD.fmk for 48 h (**b**) or 24 h (**c**). Cell viability was determined by ATP assay. Numbers represent viability normalized to that of the compound-treated cells in the absence of TNFα. Error bars, s.d. (**d**) Structures of the selected Nec-1 derivatives.

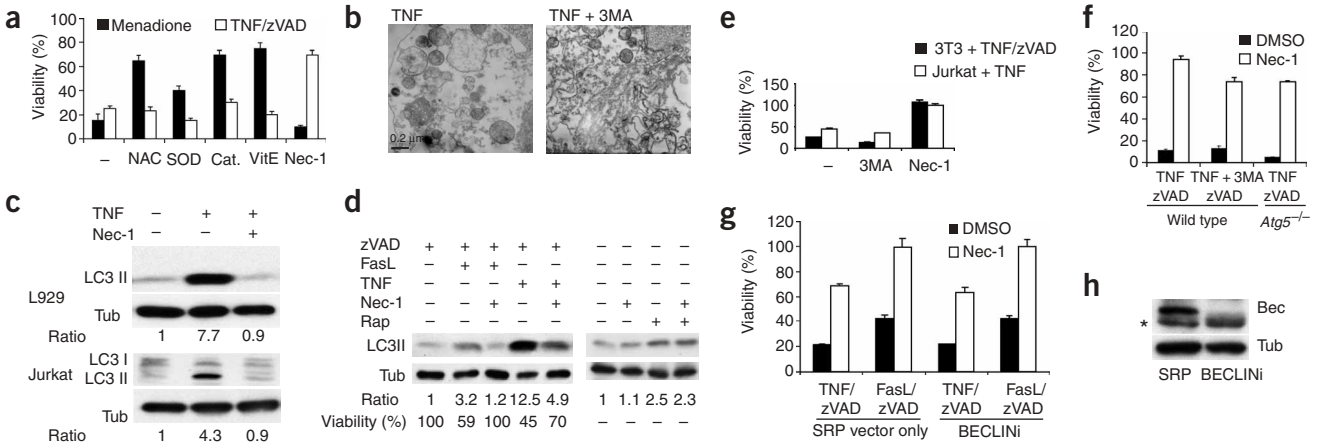

Figure 4 Roles of oxidative stress and autophagy in necroptosis. (**a**) Necroptosis is distinguishable from oxidative stress-induced cell death. U937 cells were treated with 40 ng ml^{-1} human TNFα and zVAD.fmk for 72 h or 250 μM of menadione for 24 h in the presence of various antioxidants and 100 μM Nec-1. In this and subsequent panels cell viability was determined via ATP assay. Numbers represent viability normalized to that of the DMSO-treated cells in the absence of TNFα and menadione. Throughout, error bars represent s.d. (**b**) Electron microscopic detection of autophagosomes in FADD-deficient Jurkat cells treated with TNFα with or without 10mM 3MA for 12 h. Representative images are shown. (**c**) Induction of LC3-II during necroptosis in L929 and FADD-deficient Jurkat cells treated with TNFα and Nec-1 for 8 and 24 h, respectively. Protein lysates were subjected to western blotting with antibodies to LC3 and to tubulin. The ratio of LC3-II to tubulin signals was calculated ('Ratio') and normalized to the value in the control sample. (**d**) Induction of LC3-II during necroptosis in BALB/c 3T3 cells treated with TNFα-zVAD.fmk or FasL-zVAD.fmk and Nec-1 for 24 h. Alternatively, cells were treated with 2 μM rapamycin. (**e**–**g**) No inhibition of necroptosis by suppression of autophagy in BALB/c 3T3 (**e**), FADD-deficient Jurkat (**e**), *Atg5*$^{-/-}$ MEFs (**f**) and beclin-1 RNAi–expressing BALB/c3T3 (**g**) cells. Cells were treated with TNFα-zVAD.fmk and 3MA or Nec-1 for 24 or 30 (Jurkat cells) h. Numbers represent viability normalized to that of the compound-treated cells in the absence of TNFα. (**h**) Expression of beclin-1 ('Bec') and tubulin ('Tub') in the stable populations of cells in **g** was analyzed by western blotting. Asterisk shows nonspecific band detected by antibody to beclin.

known biological activities (BIOMOL ICCB Known Bioactives library; http://iccb.med.harvard.edu) and found that no compound could block necroptosis in all cell types, as does Nec-1 (data not shown). These results underscore the unique nature of necroptosis regulation and Nec-1 activity.

Oxidative stress has been suggested as having a role in DR-induced caspase-independent cell death in some cell types, including U937 and L929 (ref. 17). However, we found that only a small fraction of TNFα-treated necroptotic FADD-deficient Jurkat cells showed an increase in ROS (~30% of dying cells; see **Supplementary Fig. 1**), whereas necroptosis triggered by FADD dimerization was not accompanied by oxidative stress (data not shown), as previously reported[4]. Consistent with this observation, necroptosis in Jurkat cells was not inhibited by the antioxidant BHA (data not shown and ref. 4), nor did any chemical from a panel of general antioxidants protect U937 cells from necroptosis (**Fig. 4a**), despite the reported protection by BHA in this cell type[17]. Conversely, Nec-1 did not block the 'classic' oxidative stress-induced necrosis caused by menadione (**Fig. 4a**). From these results, we concluded that oxidative stress, although important in some systems, does not play a universal role in necroptotic signaling and that Nec-1 does not act as antioxidant in inhibiting necroptosis.

Activation of autophagy by necroptotic signaling

Autophagy, a large-scale protein degradation and catabolic mechanism[18], has been implicated in caspase-independent cell death[19], although its functional role remains a subject of debate. The EM analysis of necroptotic Jurkat cells demonstrated the presence of double membrane-enclosed vesicles filled with electron-dense material (**Fig. 4b**), which are indicative of autophagy[20]. We therefore further investigated the role of autophagy in necroptosis. We used the appearance of the phosphatidylethanolamine (PE)-conjugated form of microtubule-associated protein 1 light chain 3 (LC3-II) as a marker of autophagy, as it has been shown to play an early and critical role in the formation of the autophagosomes[21]. Indeed, autophagy, as indicated by the increase in the levels of LC3-II, was induced in a number of necroptotic systems, including FADD-deficient Jurkat cells and L929 cells treated with TNFα (**Fig. 4c**), BALB/c 3T3 cells treated with TNFα-zVAD.fmk or FasL-zVAD.fmk (**Fig. 4d**), and U937 cells treated with TNFα-zVAD.fmk (data not shown). Whereas the production of LC3-II results from a multistep process, including the cleavage of the LC3 to the LC3-I form followed by its conjugation to PE[21], we did not detect the intermediate LC3-I species in every cell type examined; this suggests that it may be rapidly processed into LC3-II in some contexts. However, necroptosis proceeded normally in the presence of 3-methyladenine (3MA), an inhibitor of autophagy (**Fig. 4e** and data not shown), in autophagy-deficient *Atg5*$^{-/-}$ MEF cells[22] (**Fig. 4f**) and in cells where the critical autophagic factor beclin-1 (ref. 23) was knocked down by RNAi (**Fig. 4g**,**h**). These results establish autophagy as a common downstream consequence of necroptosis, rather than a contributing factor to necroptotic cell death. On the other hand, although inhibition of autophagy had no effect on the final demise of Jurkat cells, it resulted in the marked accumulation of electron-dense cytoplasmic material (**Fig. 4b**), indicating a failure to remove cellular debris. Notably, whereas the treatment with Nec-1 efficiently blocked the necroptotic LC3-II induction as well as the formation of autophagic vesicles (**Figs. 2f** and **4c**,**d**), it had no effect on the LC3-II induction caused by rapamycin, a classical inducer of autophagy (**Fig. 4d**), a result indicating that Nec-1 inhibits a necroptotic signaling step upstream of autophagy but does not inhibit autophagy *per se*.

Inhibition of RIP-induced necroptosis by necrostatin

Previous analyses[6] have suggested that the kinase activity of the DR-interacting protein RIP serves as a bifurcation point separating

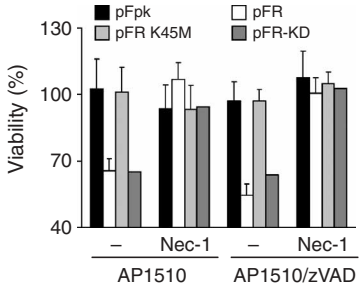

Figure 5 Nec-1 inhibits RIP kinase–induced necroptosis. FADD-deficient Jurkat cells were transiently electroporated with pEGFP and vectors encoding the FKBP12-based dimerization domain alone (pFpk) or fused to RIP (pFR), a kinase-inactive K45M mutant of RIP (pFR K45M), and kinase domain of RIP (pFR-KD) and treated 6 h later with dimerizer AP1510 without or with zVAD.fmk and Nec-1 for 48 h. Percentage of PI-negative, GFP-positive cells ('Viability, %') was determined by FACS. Numbers represent viability normalized to that of the compound-treated cells in the absence of dimerizer. Error bars, s.d.

necroptosis from other DR-dependent pathways. Indeed, dimerized full-length RIP or its kinase domain alone is sufficient to induce kinase-dependent necroptotic cell death[6], which was inhibited by Nec-1 (**Fig. 5**); this result confirmed that Nec-1 specifically affects the necroptotic branch of DR signaling. Taken together, our results demonstrate that Nec-1 targets a critical common necroptotic step downstream of DRs but upstream of a number of execution events, including mitochondrial dysfunction, loss of plasma membrane integrity and autophagic clearance of cellular debris.

Necroptosis contributes to ischemic neuronal injury

The stringent specificity of Nec-1 in inhibiting necroptosis prompted us to use it to explore the previously unknown role of necroptosis *in vivo*. Neuronal cell death caused by ischemic injury is known to contain a substantial nonapoptotic component[14,24], and the involvement of DRs in the ischemic brain injury has been suggested[25–27]. Therefore, we hypothesized that ischemic brain injury may create conditions that are nonoptimal for apoptosis but suitable for necroptosis.

To examine the involvement of necroptosis in ischemic brain injury, we determined the effect of Nec-1 on ischemic damage resulting from middle cerebral artery occlusion (MCAO) in mice. Intracerebroventricular administration of Nec-1 significantly ($P < 0.05$) reduced the infarct volume after MCAO, which suggested that necroptosis could be involved in this form of pathologic death (**Fig. 6a**). For more detailed analyses, we switched to 7-Cl-Nec-1, which showed greater activity *in vitro*. 7-Cl-Nec-1 also provided a significant ($P < 0.05$) and dose-dependent reduction in the infarct volume and a proportionate improvement in the neurological score after MCAO (**Fig. 6b**).

We next examined the specificity of 7-Cl-Nec-1 activity *in vivo*. Consistent with the specificity of Nec-1 in blocking necroptosis but not apoptosis *in vitro*, treatment with 7-Cl-Nec-1 did not block caspase-3 activation during ischemic brain injury, whereas zVAD.fmk did (**Fig. 6c**). Furthermore, coadministration of zVAD.fmk and 7-Cl-Nec-1 resulted in a significant ($P < 0.05$) additive effect (**Supplementary Fig. 3** online), though extensive optimization would be required to assess the full extent of neuroprotection by the combination treatment. In addition, 7-Cl-Nec-1 did not affect blood oxygen and CO_2 levels, body temperature or cerebral blood flow (data not

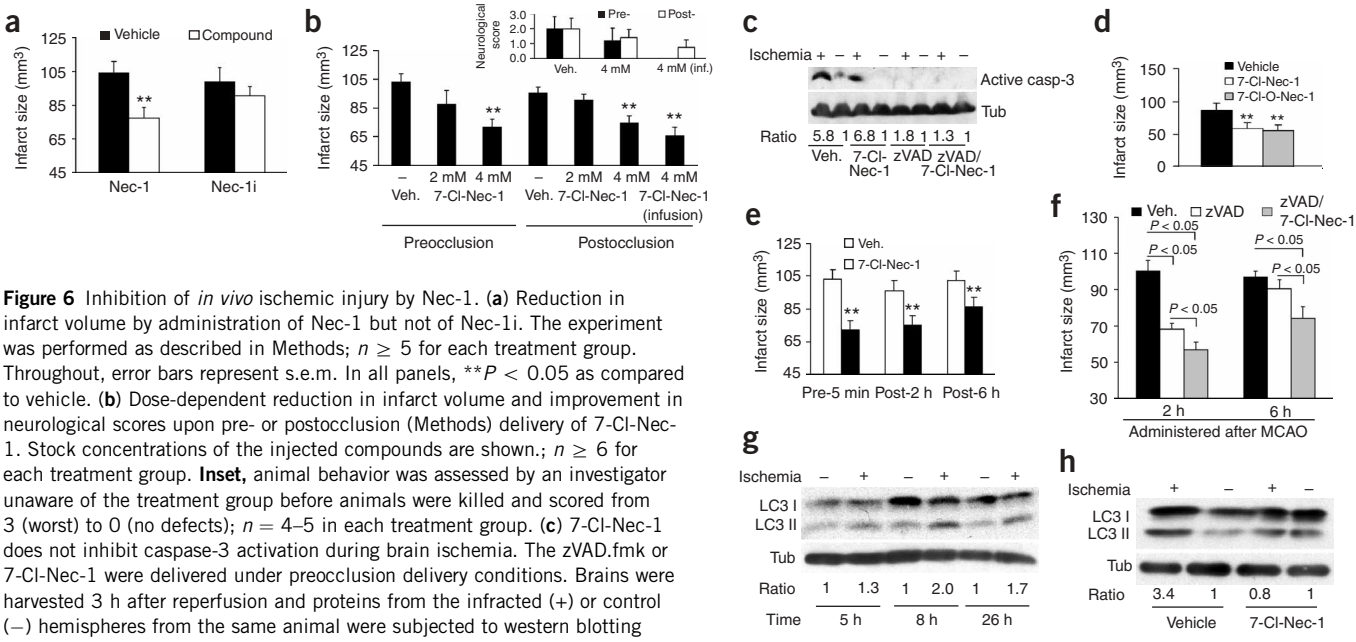

Figure 6 Inhibition of *in vivo* ischemic injury by Nec-1. (**a**) Reduction in infarct volume by administration of Nec-1 but not of Nec-1i. The experiment was performed as described in Methods; $n \geq 5$ for each treatment group. Throughout, error bars represent s.e.m. In all panels, $^{**}P < 0.05$ as compared to vehicle. (**b**) Dose-dependent reduction in infarct volume and improvement in neurological scores upon pre- or postocclusion (Methods) delivery of 7-Cl-Nec-1. Stock concentrations of the injected compounds are shown.; $n \geq 6$ for each treatment group. **Inset,** animal behavior was assessed by an investigator unaware of the treatment group before animals were killed and scored from 3 (worst) to 0 (no defects); $n = 4–5$ in each treatment group. (**c**) 7-Cl-Nec-1 does not inhibit caspase-3 activation during brain ischemia. The zVAD.fmk or 7-Cl-Nec-1 were delivered under preocclusion delivery conditions. Brains were harvested 3 h after reperfusion and proteins from the infracted (+) or control (−) hemispheres from the same animal were subjected to western blotting using antibodies to active caspase-3 or to tubulin. The ratio of caspase-3 to tubulin signals was calculated and normalized to the values in the corresponding control hemispheres. (**d**) 7-Cl-O-Nec-1 has activity comparable to that of 7-Cl-Nec-1 *in vivo*. Mice were injected with 7-Cl-Nec-1 or 7-Cl-O-Nec-1 at 4 and 6 h postocclusion; $n \geq 10$ in each treatment group. (**e**) Establishing the therapeutic time window of 7-Cl-Nec-1 in MCAO model by injecting compound either 5 min before or immediately after 2-h MCAO at 2, 4 or 6 h postocclusion; $n \geq 10$ in each treatment group. (**f**) Lack of neuroprotection by zVAD.fmk upon administration 6 h postocclusion. The delivery of compounds was performed at 2 h, 4 h or 6 h after the onset occlusion; $n \geq 8$ in each treatment group. *P* values are shown. (**g**) Delayed induction of LC3-II during brain ischemia *in vivo*. Brains were harvested at indicated time points after occlusion and subjected to western blotting with antibodies to LC3 and to tubulin. LC3-II/tubulin ratio is shown. (**h**) Inhibition of late induction of LC3-II by delayed administration of 7-Cl-Nec-1 at 4 and 6 h after occlusion. Brains were collected 8 h after occlusion and analyzed as in **g**.

shown), which indicated that it does not prevent ischemic cell death through a nonspecific effect on general physiology.

To confirm the mode of action of Nec-1 *in vivo*, we performed a structure-activity relationship analysis of its protection against ischemic brain injury. First, Nec-1i, an inactive derivative of Nec-1 that lacks a single methyl group (**Fig. 3d**), did not significantly affect infarct volume (**Fig. 6a**). Second, 7-Cl-O-Nec-1 (**Fig. 3d**), possessing antinecroptotic activity *in vitro* similar to that of 7-Cl-Nec-1 (**Fig. 3d**), showed activity indistinguishable from that of 7-Cl-Nec-1 *in vivo* (**Fig. 6d**). These data demonstrate a strict correlation between the inhibition of necroptosis *in vitro* and the anti-ischemic activity of 7-Cl-Nec-1 *in vivo*, providing strong support for our hypothesis that neuroprotection by Nec-1 is accomplished through the inhibition of necroptosis.

Notably, the protective effect of 7-Cl-Nec-1 was readily detectable even when the compound was administered 6 h after the onset of injury (**Fig. 6e**), at which point the administration of zVAD.fmk no longer reduces infarct volume[28] (**Fig. 6f**). We reasoned that this extended time window of neuroprotection by 7-Cl-Nec-1 *in vivo* might reflect a delayed induction of necroptosis during ischemic brain injury. To verify this hypothesis, we analyzed the induction of LC3-II during MCAO, as our *in vitro* analyses suggested that this event is associated with necroptosis. We observed that although LC3-II was clearly induced after ischemic brain injury, it did not reach the maximal level until 8 h postocclusion (**Fig. 6g**). Furthermore, delayed injection of 7-Cl-Nec-1 at 4 and 6 h postocclusion still efficiently blocked the LC3-II increase at the 8-h time point (**Fig. 6h**), confirming that the late induction of LC3-II *in vivo* indeed reflects the delayed activation of necroptosis.

DISCUSSION

Nec-1 provides a powerful tool for characterizing the role of necroptosis *in vitro* and *in vivo*. We showed that necroptosis represents a common, alternative cell-death pathway triggered by DR signaling in multiple cell types and established its physiological relevance *in vivo* as a delayed component of ischemic brain injury. We showed that, in addition to the early and simultaneous loss of cytoplasmic membrane integrity and mitochondrial membrane potential, which had been observed previously[4–6], necroptosis also involves the activation of autophagy, probably as a self-clearance mechanism. Our study extends the conventional use of small molecules in biology, which aims to characterize specific functions of their direct targets, to a broader level of defining new biological pathways.

Our data suggest that although necroptosis shares some features with all three major established mechanisms of cell death, that is, apoptosis, necrosis or type 2 autophagic death[29], it represents a previously unknown and distinct form of cell death. Although the same death receptor agonist may trigger necroptosis and apoptosis, necroptosis can be differentiated from apoptosis both morphologically and functionally. Furthermore, although necroptosis shares some morphological features of necrosis, it is distinguishable from the latter by being an active cell death triggered by DR signaling, rather than nonspecific cellular injury.

Autophagy has a dual role as an intrinsic cell-death mechanism under some circumstances[23] and as a cell-survival pathway under others[30]. We showed that although autophagy is commonly induced by necroptosis, this mechanism is not critical for cellular demise. Thus, autophagy is a cellular response to necroptosis, rather than a part of the death execution mechanism *per se*. Furthermore, Nec-1 blocks necroptosis but not rapamycin-induced autophagy (**Fig. 4d**), which indicates that the two processes are independently regulated. Although we cannot exclude the possibility that in some instances autophagy might contribute more actively to the execution of necroptosis, our data clearly show that, in general, necroptosis is functionally distinguishable from autophagy and does not depend on autophagy for cell-death execution.

Necroptosis does not appear to involve any previously described factors implicated in caspase-independent cell death, and Nec-1 clearly shows a unique ability in inhibiting necroptotic death as compared with other known biologically active molecules. Although definitive confirmation and full characterization of the necroptosis pathway must await the identification of the Nec-1 binding target(s), which is a subject of ongoing investigation, the unique selectivity of Nec-1 in blocking necroptosis suggests that its target may be a factor previously unknown as a regulator of nonapoptotic cell death.

Our results demonstrate the role of necroptosis as a mechanism of delayed ischemic brain injury, providing the first example of active necrotic cell death *in vivo*. The slow-onset kinetics of necroptosis *in vitro* and *in vivo* suggest the intriguing possibility that this pathway might provide a new target for neuroprotective intervention with an extended therapeutic window. A limited therapeutic window has been one of the major factors in the failure of several antistroke drug candidates in clinical trials[31]. On the other hand, the therapeutic time window of 7-Cl-Nec-1 exceeds that of most other compounds found previously to work in the MCAO model, including inhibitors of PARP, a known nonapoptotic death regulator[32,33].

The exact stimulus that activates necroptosis in ischemic brain injury is currently unknown. Although we do not exclude the possibility that other pro-death signals might activate necroptosis in ischemic neurons and other conditions, we speculate that the activation of DRs by FasL and TNFα contributes to the activation of necroptosis during ischemic brain injury, because the induction of FasL and TNFα and the activation of DRs have been shown to contribute to ischemic and traumatic brain injury[26,34]. Furthermore, we hypothesize that the temporal course of upregulation of FasL, TNFα and other DR ligands' expression in ischemic brain injury may contribute to the delayed induction of necroptosis *in vivo*, which suggests that continuous administration of Nec-1 might provide additional neuroprotective benefits.

Necroptosis may function as a cellular 'backup' mechanism to ensure the elimination of damaged cells under stress conditions when apoptosis is inhibited. The slow-onset kinetics of necroptosis are consistent with this proposal. Furthermore, although our data suggest that neuronal necroptosis can occur under ischemic conditions without exogenous caspase inhibitors, it may still reflect the failure to undergo apoptosis in some parts of the ischemic brain. This may result from the development of an apoptosis-nonpermissive environment upon ischemic injury owing, for example, to insufficient cellular energy supplies, as the level of cellular ATP is a critical determinant for cells in undergoing apoptosis or necrosis[35]. Alternatively, it is also possible that necroptosis may function as the primary cell death mechanism in a subpopulation of neurons. Future studies are needed to distinguish among these possibilities.

Finally, although our study specifically explored the role of necroptosis in ischemic brain injury as a proof-of-principle example system, the demonstration of an intrinsic necrotic cell-death mechanism suggests the broader possibility of specifically targeting necrosis as a therapeutic strategy in other contexts. Indeed, there is extensive evidence that necrotic cell death plays a prominent role in a wide range of human pathological conditions, such as myocardial infarction and acute and chronic neurodegeneration[36,37]. The availability of Nec-1 offers a unique opportunity to characterize the role of necroptosis in these and other human pathologies.

METHODS

Antibodies and reagents. FasL (used at 10 ng ml^{-1}) and zVAD.fmk (used at 100 μM) were from Alexis Biochemicals. Human or mouse (used for MEF cells) TNFα (used at 10 ng ml^{-1}) was from Cell Sciences. Sytox Green, TO-PRO-3 and $DiOC_6$ were from Molecular Probes. Propidium iodide was from Roche. The dimerizing agents AP1510 and AP20187 (both used at 100 nM) were obtained from Ariad Pharmaceuticals. CHX (used at 1 μg ml^{-1}), antioxidants (*N*-acetyl cysteine (NAC), used at 2.5 mM; superoxide dismutase (SOD), 800 U ml^{-1}; catalase (cat.), 1,400 U ml^{-1}; vitamin E (vit. E), 5 mM), phalloidin-TRITC and all common chemicals were from Sigma. The following antibodies were used: mouse anti–β-tubulin (Stressgen), rabbit anti-LC3 (ref. 20), rabbit anti–beclin-1 (Santa Cruz), rabbit anti-giantin (Covance), mouse anti-KDEL (Stressgen) and mouse anti–cytochrome *c* (Pharmingen). Secondary horseradish peroxidase (HRP)-conjugated antibodies were from Southern Biotech. Secondary Alexa 488–conjugated antibodies were from Molecular Probes; Cy3-conjugated antibodies were from Jackson ImmunoResearch.

Preparation and use of Nec-1 and its derivatives. For details of chemical synthesis see **Supplementary Methods**. We used compounds at 30 μM in all cellular assays unless otherwise indicated.

Chemical screening. We plated U937 cells in 384-well plates at 5,000–10,000 cells per well in 40-μl phenol red–free RPMI 1640 medium containing 100 μM zVAD.fmk and 40 ng ml^{-1} human TNFα using a Multidrop dispenser (Thermo Electron). We added 100 nl of the DiverSetE (5 mg ml^{-1} in DMSO, Chembridge) using a Seiko-based custom-built pin transfer robot (Institute of Chemistry and Cell Biology, Harvard Medical School). After 72 h, we assessed cell viability using a luminescence-based ATP assay (ATPLite-M, PerkinElmer). We also dispensed cells not treated with TNFα in each plate as a positive control. We purchased Nec-1 and other preliminary positive hits (not described) from Chembridge for individual retesting.

Cell viability assays. We seeded cells in 96-well plates (white plates for luminescent assays; black plates for fluorescent assays; clear plates for MTT assay) at the density of 5,000–10,000 cells per well for adherent cells or 20,000–50,000 cells per well for suspension cells in 100 μl of the appropriate phenol red–free media. After incubation, we determined cell viability using one of the following methods. For the ATP assay, we used luminescence-based commercial kits (CellTiter-Glo, Promega or ATPLite-M, PerkinElmer) and analyzed luminescence using a Wallac Victor II plate reader (PerkinElmer). For Sytox assay, we incubated cells with 1 μM Sytox Green reagent for 30 min at 37 °C, and then performed fluorescent reading. Subsequently, we added 5 μl of 20% Triton X-100 solution into each well to produce maximal lysis and incubated cells for 1 h at 37 °C, then performed the second reading. We calculated the ratio of values (percentage of dead cells in each well) before and after Triton treatment and normalized it to the relevant controls not subjected to cytotoxic stimuli, as indicated in figure legends. For the MTT assay, we used the CellTiter 96 AQ_{ueous} Non-Radioactive Cell Proliferation Assay kit (Promega). For PI exclusion assays, we added 2 μg ml^{-1} PI into the medium and immediately analyzed samples using FACSCalibur (BD Biosciences). For PI–annexin V assay we used the ApoAlert Annexin V-EGFP Apoptosis Kit (Clontech). For $DiOC_6$ staining, we incubated cells with 40 nM $DiOC_6$ for 30 min at 37 °C, washed once and analyzed in FACSCalibur. For ROS analysis, we incubated cells with 5 μM dihydroethidium (Molecular Probes) for 30 min at 37 °C, washed once and analyzed in FACSCalibur. EM analyses were performed at the Harvard Medical School EM facility. We acquired bright-field images of the cells using an Axiovert 200 microscope (Zeiss).

Transient focal cerebral ischemia in the mouse. The animal protocol was approved by the Massachusetts General Hospital Subcommittee on Animal Research Care that serves as the Institutional Animal Care and Use Committee, and all procedures were performed in accordance with the Public Health Service Policy on Humane Care and Use of Laboratory Animals. Animals were maintained in accordance with the "Guide for the Care and Use of Laboratory Animals" (National Research Council, 1996). We anesthetized spontaneously breathing adult male SV-129 mice (19–23 g; Taconic Farms) with 2% isoflurane and maintained them on 0.8–1% isoflurane in 70% N_2O and 30% O_2 using a Fluotec 3 vaporizer (Colonial Medical). We occluded the left MCA with an intraluminal 8-0 nylon monofilament (Ethicon) coated with a mixture of silicone resin (Xantopren, Bayer Dental) and a hardener (Elastomer Activator, Bayer Dental). The procedure lasted 15 min, and the anesthesia was discontinued. We briefly reanesthetized animals 2 h later with isoflurane, and withdrew the filament. Eighteen hours after reperfusion we divided forebrains into five coronal (2-mm) sections using a mouse brain matrix (RBM-2000C; Activational Systems), and stained the sections with 2% 2,3,5-triphenyltetrazolium chloride (Sigma). We quantified infarct areas using an image-analysis system (Bioquant IV, R & M Biometrics) and calculated infarct volume directly by adding the infarct volume in each section.

For drug administration, we dissolved 7-Cl-Nec-1 or other derivatives in 4% methyl-β-cyclodextrin (Sigma) solution in PBS and administered it through intracerebroventricular administration at the time points indicated. Typically, we performed two 2-μl injections of 4 mM stock solution (unless otherwise indicated). For preocclusion delivery, we performed injections 5 min before the onset of 2-h MCAO occlusion and immediately after the cessation of the occlusion, at the time of the reperfusion. For postocclusion delivery, we performed injections at the time of reperfusion after 2 h of MCAO as well as 2 h after the onset of reperfusion. In the case of infusion, we infused 20 μl of compound over a 30-min time period. In the case of injection 6 h after occlusion, we injected a single 4-μl dose. In the case of zVAD.fmk administration, we added it to the Nec-1 formulation and administered a total dose of 160 ng.

Note: Supplementary information is available on the Nature Chemical Biology website.

ACKNOWLEDGMENTS

This work was supported in part by grants from the US National Institute of General Medicine (R01 GM64703) and National Institute on Aging (R37 AG012859) to J.Y., the National Institute of Neurological Disorders and Stroke (R01 NS37141-08) to M.M. and J.Y., and funding from the Harvard Center for Neurodegeneration and Repair to G.D.C. A.D. is a recipient of a National Institute on Aging Mentored Research Scientist Career Development Award and an American Health Assistance Foundation Pilot Award. We thank X. Teng for help in preparing compounds for animal testing; M. Lipinski and R. Olea-Sanchez for critical reading of the manuscript; C. Ayata for helpful suggestions with MCAO experiments; and G. Nunez, T. Jacks, J. Blenis and T. Yoshimori for providing RIP constructs, pSRP vector and mutant Jurkat cells, and anti-LC3 antibody, respectively.

COMPETING INTERESTS STATEMENT

The authors declare that they have no competing financial interests.

Received 10 February; accepted 10 May 2005
Published online at http://www.nature.com/naturechemicalbiology/

1. Degterev, A., Boyce, M. & Yuan, J. A decade of caspases. *Oncogene* **22**, 8543–8567 (2003).
2. Wallach, D. *et al.* Tumor necrosis factor receptor and Fas signaling mechanisms. *Annu. Rev. Immunol.* **17**, 331–367 (1999).
3. Vercammen, D. *et al.* Dual signaling of the Fas receptor: initiation of both apoptotic and necrotic cell death pathways. *J. Exp. Med.* **188**, 919–930 (1998).
4. Matsumura, H. *et al.* Necrotic death pathway in Fas receptor signaling. *J. Cell Biol.* **151**, 1247–1256 (2000).
5. Schulze-Osthoff, K., Krammer, P.H. & Droge, W. Divergent signalling via APO-1/Fas and the TNF receptor, two homologous molecules involved in physiological cell death. *EMBO J.* **13**, 4587–4596 (1994).
6. Holler, N. *et al.* Fas triggers an alternative, caspase-8-independent cell death pathway using the kinase RIP as effector molecule. *Nat. Immunol.* **1**, 489–495 (2000).
7. Chan, F.K. *et al.* A role for tumor necrosis factor receptor-2 and receptor-interacting protein in programmed necrosis and antiviral responses. *J. Biol. Chem.* **278**, 51613–51621 (2003).
8. Kawahara, A., Ohsawa, Y., Matsumura, H., Uchiyama, Y. & Nagata, S. Caspase-independent cell killing by Fas-associated protein with death domain. *J. Cell Biol.* **143**, 1353–1360 (1998).
9. Khwaja, A. & Tatton, L. Resistance to the cytotoxic effects of tumor necrosis factor alpha can be overcome by inhibition of a FADD/caspase-dependent signaling pathway. *J. Biol. Chem.* **274**, 36817–36823 (1999).
10. Lin, Y. *et al.* Tumor necrosis factor-induced nonapoptotic cell death requires receptor-interacting protein-mediated cellular reactive oxygen species accumulation. *J. Biol. Chem.* **279**, 10822–10828 (2004).
11. Ruemmele, F.M., Dionne, S., Levy, E. & Seidman, E.G. TNFα-induced IEC-6 cell apoptosis requires activation of ICE caspases whereas complete inhibition of the caspase cascade leads to necrotic cell death. *Biochem. Biophys. Res. Commun.* **260**, 159–166 (1999).

12. Wilson, C.A. & Browning, J.L. Death of HT29 adenocarcinoma cells induced by TNF family receptor activation is caspase-independent and displays features of both apoptosis and necrosis. *Cell Death Differ.* **9**, 1321–1333 (2002).
13. Nieminen, A.L. Apoptosis and necrosis in health and disease: role of mitochondria. *Int. Rev. Cytol.* **224**, 29–55 (2003).
14. Lo, E.H., Dalkara, T. & Moskowitz, M.A. Mechanisms, challenges and opportunities in stroke. *Nat. Rev. Neurosci.* **4**, 399–415 (2003).
15. Li, M. & Beg, A.A. Induction of necrotic-like cell death by tumor necrosis factor α and caspase inhibitors: novel mechanism for killing virus-infected cells. *J. Virol.* **74**, 7470–7477 (2000).
16. Kain, S.R. & Ma, J.T. Early detection of apoptosis with annexin V-enhanced green fluorescent protein. *Methods Enzymol.* **302**, 38–43 (1999).
17. Fiers, W., Beyaert, R., Declercq, W. & Vandenabeele, P. More than one way to die: apoptosis, necrosis and reactive oxygen damage. *Oncogene* **18**, 7719–7730 (1999).
18. Klionsky, D.J. & Emr, S.D. Autophagy as a regulated pathway of cellular degradation. *Science* **290**, 1717–1721 (2000).
19. Gozuacik, D. & Kimchi, A. Autophagy as a cell death and tumor suppressor mechanism. *Oncogene* **23**, 2891–2906 (2004).
20. Kabeya, Y. *et al.* LC3, a mammalian homologue of yeast Apg8p, is localized in autophagosome membranes after processing. *EMBO J.* **19**, 5720–5728 (2000).
21. Kabeya, Y. *et al.* LC3, GABARAP and GATE16 localize to autophagosomal membrane depending on form-II formation. *J. Cell Sci.* **117**, 2805–2812 (2004).
22. Kuma, A. *et al.* The role of autophagy during the early neonatal starvation period. *Nature* **432**, 1032–1036 (2004).
23. Yu, L. *et al.* Regulation of an ATG7-beclin-1 program of autophagic cell death by caspase-8. *Science* **304**, 1500–1502 (2004).
24. Gwag, B.J., Lobner, D., Koh, J.Y., Wie, M.B. & Choi, D.W. Blockade of glutamate receptors unmasks neuronal apoptosis after oxygen-glucose deprivation *in vitro*. *Neuroscience* **68**, 615–619 (1995).
25. Rosenbaum, D.M. *et al.* Fas (CD95/APO-1) plays a role in the pathophysiology of focal cerebral ischemia. *J. Neurosci. Res.* **61**, 686–692 (2000).
26. Martin-Villalba, A. *et al.* CD95 ligand (Fas-L/APO-1L) and tumor necrosis factor-related apoptosis-inducing ligand mediate ischemia-induced apoptosis in neurons. *J. Neurosci.* **19**, 3809–3817 (1999).
27. Martin-Villalba, A. *et al.* Therapeutic neutralization of CD95-ligand and TNF attenuates brain damage in stroke. *Cell Death Differ.* **8**, 679–686 (2001).
28. Endres, M. *et al.* Attenuation of delayed neuronal death after mild focal ischemia in mice by inhibition of the caspase family. *J. Cereb. Blood Flow Metab.* **18**, 238–247 (1998).
29. Kitanaka, C. & Kuchino, Y. Caspase-independent programmed cell death with necrotic morphology. *Cell Death Differ.* **6**, 508–515 (1999).
30. Lum, J.J. *et al.* Growth factor regulation of autophagy and cell survival in the absence of apoptosis. *Cell* **120**, 237–248 (2005).
31. Richard Green, A., Odergren, T. & Ashwood, T. Animal models of stroke: do they have value for discovering neuroprotective agents? *Trends Pharmacol. Sci.* **24**, 402–408 (2003).
32. Takahashi, K. & Greenberg, J.H. The effect of reperfusion on neuroprotection using an inhibitor of poly(ADP-ribose) polymerase. *Neuroreport* **10**, 2017–2022 (1999).
33. Abdelkarim, G.E. *et al.* Protective effects of PJ34, a novel, potent inhibitor of poly(ADP-ribose) polymerase (PARP) in *in vitro* and *in vivo* models of stroke. *Int. J. Mol. Med.* **7**, 255–260 (2001).
34. Matsuyama, T. *et al.* Fas antigen mRNA induction in postischemic murine brain. *Brain Res.* **657**, 342–346 (1994).
35. Eguchi, Y., Shimizu, S. & Tsujimoto, Y. Intracellular ATP levels determine cell death fate by apoptosis or necrosis. *Cancer Res.* **57**, 1835–1840 (1997).
36. McCully, J.D., Wakiyama, H., Hsieh, Y.J., Jones, M. & Levitsky, S. Differential contribution of necrosis and apoptosis in myocardial ischemia-reperfusion injury. *Am. J. Physiol. Heart Circ. Physiol.* **286**, H1923–H1935 (2004).
37. Yuan, J., Lipinski, M. & Degterev, A. Diversity in the mechanisms of neuronal cell death. *Neuron* **40**, 401–413 (2003).

CORRIGENDUM: Chemical inhibitor of nonapoptotic cell death with therapeutic potential for ischemic brain injury

Alexei Degterev, Zhihong Huang, Michael Boyce, Yaqiao Li, Prakash Jagtap, Noboru Mizushima, Gregory D Cuny, Timothy J Mitchison, Michael A Moskowitz & Junying Yuan
Nat. Chem. Biol. **1**, 112–119 (2005)

In the legend to **Supplementary Figure 1** online, the second sentence in panel **d** should read "FADD-deficient Jurkat cells were treated with indicated concentrations (on log scale, in μM) of Nec-1 (**1**) and Nec-1i (**2**) for 24 h."

ERRATUM: Small-molecule interaction with a five-guanine-tract G-quadruplex structure from the human *MYC* promoter

Anh Tuân Phan, Vitaly Kuryavyi, Hai Yan Gaw & Dinshaw J Patel
Nat. Chem. Biol. **1**, 167–173 (2005)
In **Table 1**, footnote 'a' should read: "[a]Modifications in sequences derived from *Pu24* are underlined."